Volcanic–plutonic connections in a tilted nested caldera complex in Hong Kong

Roderick J. Sewell[1], Denise L.K. Tang[1], and S. Diarmad G. Campbell[2]

[1]Hong Kong Geological Survey, Geotechnical Engineering Office, Civil Engineering and Development Department, 101 Princess Margaret Road, Kowloon, Hong Kong SAR, China

[2]British Geological Survey, Murchison House, West Mains Road, Edinburgh, EH9 3LA, UK

ABSTRACT

Exceptional exposures of four, precisely-dated, Middle Jurassic to Early Cretaceous, silicic volcanic centers and their plutonic equivalents in Hong Kong have provided an excellent opportunity to examine close connections in time and space between magma chambers and their overlying calderas. Here, we describe a ~14 km crustal section through a collapsed caldera in southeastern Hong Kong where the intracaldera fill suggests that the magmatic discharge was of supereruption scale. The main subvolcanic components that link a magma chamber with surface are revealed by well-established field relationships, supplemented by high precision geochronology, whole-rock geochemistry, and geophysical data. Exposures and outcrop patterns reveal kilometer-scale caldera subsidence and evidence of the simultaneous evacuation of hundreds of cubic kilometers of high-silica rhyolite magma through dike-like conduits from a shallow subcrustal reservoir. The resultant volcanotectonic depression, within which is preserved a single cooling unit of massively columnar-jointed densely welded tuff (High Island tuff), is interpreted to form part of a larger tilted Early Cretaceous nested caldera complex. The High Island eruption signaled the end of a 24 Myr-period of voluminous, pulsed Middle Jurassic to

Early Cretaceous silicic magmatism in the Hong Kong region characterized by four discrete ignimbrite 'flare-ups'.

1. Introduction

Primary investigative methods of the geometry of magmatic plumbing systems beneath large silicic calderas generally concentrate on geophysical measurements of giant caldera complexes in repose [e.g., *Christiansen et al*., 2007], geochemical and structural studies of exhumed subvolcanic magma chambers [e.g., *Kokelaar and Moore*, 2006], and detailed petrologic studies of crystals and melt inclusions in eruptive materials [e.g., *Davidson et al*., 2007]. Descriptions of near-continuous upper crustal sections, which allow direct observations of the architecture of these systems from the floor of the magma chamber to the top of the exposed caldera infill, are relatively uncommon [e.g., *Quick et al*., 2009]. Here, we describe a ~14 km crustal section through a tilted Early Cretaceous nested caldera complex in southeastern Hong Kong (herein the Special Administrative Region), whose internal architecture has been exhumed through a fortuitous combination of gentle crustal warping and erosion. The relationships of the caldera and its subvolcanic plumbing have been mapped and further deduced from geological, geochemical and geophysical evidence and established within the context of overlapping Early Cretaceous volcanic–plutonic centers. This paper lays the foundation for upcoming detailed petrologic investigations by one of us (DLKT), and particularly specific crystal studies using micro-analytical techniques, of these overlapping magmatic centers. This may help to address current controversies about the evolution of large silicic magma systems [e.g., *Coleman et al*., 2004; *Glazner et al*., 2004; *Gray et al*., 2008; *Reid et al*., 2011] and their volcanic–plutonic connections [e.g., *Bachmann et al*., 2007; *Kennedy and Stix*, 2007; *John et al*., 2008].

2. Geologic Setting

Over 80% of the rocks in Hong Kong are Middle Jurassic to Early Cretaceous (Early Yanshanian 190–140 Ma) volcanic–plutonic associations. These belong to four main episodes: 165–160 Ma, 148–146 Ma, 143 Ma and 141 Ma, constrained by 44 high-precision U-Pb single crystal zircon ages [*Campbell and Sewell*, 1997; *Davis et al*., 1997, *Campbell et al*., 2007; *Sewell et al*., 2012] and approximately 1000 whole-rock major and trace element analyses [*Sewell and Campbell*, 1997; Figure 1]. The episodes are consistent with regional-scale ignimbrite 'flare-ups' (used here informally to reflect magmatic episodes of very variable duration and lateral extent). The magmatic events in Hong Kong are only a small part of the very much larger zone of Early Yanshanian magmatism that occurred at the same time in southeastern China [*Li and Li*, 2007]. High precision U-Pb zircon ages from Guangdong Province suggest that magmatic episodes were of similar timing and duration to Hong Kong. Accordingly, Hong Kong is ideally placed to constrain the episodic nature of magmatism within the zone as a whole.

The two Jurassic (165–160 Ma, 148–146 Ma) 'flare-ups' and their volcanic and subvolcanic expressions are spatially and temporally well-defined in northwestern and central Hong Kong and include volcanic–plutonic caldera complexes on Lantau Island and in the central New Territories (Figure 1). They are composed of: mainly high-K calcalkaline dacite to rhyolite lapilli to coarse ash crystal tuffs; and related I-type granitoid and A-type granite (65–72 wt% SiO_2) plutons [*Sewell et al*., 1992; *Campbell and Sewell*, 1997; *Sewell and Campbell*, 1997]. Nearly complete, NE- and E-elongated calderas, delineated by ring faults and ring-like intrusions, reflect the strong influence of NE-trending regional faults on the distribution and loci of two Jurassic volcanic centers [Figure 1, *Campbell and Sewell*, 1997].

The two Early Cretaceous (143 Ma, 141 Ma) 'flare-ups' and their volcanic and subvolcanic expressions spatially overlap in southeastern Hong Kong. They include volcanic–

plutonic caldera complexes in the eastern New Territories and southern Hong Kong Island (Figure 1). These are dominated by high-K calcalkaline to shoshonitic high silica rhyolite (>75 wt% SiO_2), welded, fine ash vitric tuff, with subordinate dacite to rhyolite coarse ash crystal tuff, and minor trachydacite to rhyolite lava [*Sewell and Campbell*, 1997]. Compositional-related and broadly coeval age-related intrusions comprise I-type granites, and A-type dikes and stocks of quartz monzonite [*Campbell and Sewell*, 1997; *Davis et al*., 1997; *Sewell and Campbell*, 1997; *Sewell et al*., 2012]. In contrast to the Jurassic calderas, the preservation of the Early Cretaceous calderas is more incomplete; they have northerly elongations consistent with movement on E- and N-trending faults.

3. Early Cretaceous Volcanic–Plutonic Coeval Episodes

In the eastern New Territories, volcanic and sedimentary rocks belonging to the two Early Cretaceous 'flare-ups' dip gently to the east at 10–30º. They are underlain in the west by subvolcanic granite plutons and quartz monzonite stocks of equivalent age and composition [Figure 2, *Sewell et al*., 2000]. General petrologic characteristics of the Early Cretaceous volcanic and plutonic rocks are given in Table 2.

3.1 143 Ma Volcanic–Plutonic Episode

The stratigraphy of the 143 Ma 'flare-up' has been uncertain due to subsequent caldera development (the 141 Ma 'flare-up'), and correlation of units on textural and compositional grounds is problematic. Earlier interpretations suggested broadly coeval eruptions from two separate calderas represented by: a dacite-rhyolite assemblage ('rhyolitic subgroup') from the Long Harbour Caldera and Sai Kung Caldera in eastern Kowloon, and a trachyte-rhyolite assemblage ('trachytic subgroup') from a presumed strongly dismembered, incomplete, 'caldera' centered on Hong Kong Island [Ap Lei Chau Caldera, *Campbell and Sewell*, 1997]. Folding of

91 the trachyte-rhyolite assemblage was interpreted to have been caused by granite intrusion [*Sewell*
92 *et al*., 2000]. The calderas are underlain by a NE-oriented ellipsoidal 143 Ma pluton north of
93 Kowloon [*Sewell et al*., 2012], and a subcircular 143 Ma pluton centered on southern Lantau
94 Island [*Davis et al*., 1997; Figure 2].

95 However, we have now used the TiO_2 versus Zr plot [Figure 3A, cf. *Campbell and*
96 *Sewell*, 1997, see Datasets DS01and DS02] to reconstruct the pre-collapse configuration and the
97 original stratigraphy for the 143 Ma 'flare-up' (Figure 4). This suggests that earlier eruptions
98 were dominated by voluminous, weakly zoned dacite–rhyolite (66–75 wt% SiO_2) coarse ash
99 crystal tuff (40–50% crystals), whereas later eruptions were dominated by trachydacite to high
100 silica rhyolite (63–77 wt% SiO_2) crystal-bearing fine ash vitric tuff. *Sewell and Campbell* [1997]
101 originally assigned these rocks to separate phases (Phases 3 and 4) of the 143 Ma magmatic
102 episode based on K_2O vs. SiO_2 and Ti vs. Zr relationships. Penultimate eruptions culminated in a
103 strongly welded fine ash vitric tuff. A 170 m-thick volcaniclastic unit overlying the welded tuff
104 represents the final accumulation in a volcanotectonic depression following the caldera-forming
105 event. The stratigraphic interpretation for the 143 Ma 'flare-up' is corroborated by
106 geochronological and geochemical studies of the Lantau Caldera on Lantau Island [Figure 1,
107 *Campbell et al*., 2007]. This caldera therefore preserves a condensed record of Middle Jurassic to
108 Early Cretaceous 'flare-ups', including a 200 m-thick stratigraphic sequence with very similar
109 age and compositional characteristics to the 143 Ma 'flare-up' from eastern New Territories and
110 southern Hong Kong Island.

111 In parallel with the 143 Ma volcanic sequences, the underlying 143 Ma plutons are also
112 strongly dismembered due to the subsequent 141 Ma caldera development. This is most vividly
113 illustrated by the NE-oriented ellipsoidal 143 Ma pluton north of Kowloon (Figure 2) which has

been offset, apparently dextrally, by approximately 4 km, along a prominent NE-trending fault marked by a 141 Ma quartz monzonite dike (Wong Chuk Fault – see below). In addition to radiometric ages and spatial associations, whole-rock geochemical relationships [*Campbell and Sewell*, 1997; *Sewell and Campbell*, 1997] demonstrate a genetic link between the 143 Ma plutonic and volcanic rocks.

3.2 141 Ma Volcanic–Plutonic Episode

The first expression of the 141 Ma 'flare-up' appears to have been extrusion of flow-banded trachydacite and eruption of rhyolite welded tuff on 143 Ma volcanic materials locally from conduits in Clear Water Bay [*Sewell et al*., 2012]. This was followed by eruption of rhyolite lava and tuff from conduits in the eastern New Territories [*Sewell et al*., 2000]. Subsequently, a caldera (High Island Caldera, Figure 2) developed during eruption and emplacement of the High Island tuff. The northern and southern boundaries of the High Island Caldera were previously delimited on the basis of E-trending and NW-trending faults, but the eastern and western boundaries were not identified [*Campbell and Sewell*, 1997]. The High Island tuff, comprising a single cooling unit of compositionally uniform, high-silica rhyolite (>75 wt% SiO_2) crystal-bearing fine ash vitric tuff [Figure 3B, cf. *Campbell and Sewell*, 1997; Figure 4], is non-welded to partly-welded at its base [*Tam and Chan*, 1983], grading rapidly upward over 30 m into densely welded tuff. The densely welded tuff (Figure 5A) is characterized by spectacularly well-developed columnar jointing, with column diameters up to 2 m (Figure 5B) and observed vertical extents of 30 m and probably more. The base of the High Island tuff rests on a 35 m-thick volcaniclastic unit characterized by tuff breccia, tuffaceous sandstone and mudstone [*Strange et al*., 1990, Figure 5C]. An outlier of 141 Ma 'flare-up' is preserved approximately 40 km to the southwest within the Lantau Caldera [*Campbell et al*., 2007]. This

outlier consists of a 230 m-thick sequence of welded tuff, flow-banded rhyolite, and tuff breccia, resting on an 80 m-thick volcaniclastic unit which separates the 141 Ma volcanic assemblage from the underlying 143 Ma volcanic assemblage (Figure 4).

The medium-grained 141 Ma granite pluton centered in Kowloon is capped along its eastern boundary by fine-grained granite which has intruded the overlying 143 Ma volcanic sequence (Figure 2). The fine-grained granite, containing miarolitic cavities, is locally strongly greisenized and mineralized at its contact with volcanic rocks. The coeval NE- to E-trending quartz monzonite to monzogranite dikes approximate the northern and southern boundaries of the medium-grained granite pluton (Figure 2).

In northern Kowloon, the dikes commonly occur as broad (10 to 100 m wide) composite (quartz monzonite to porphyritic monzogranite) intrusions. These amalgamate eastwards into stocks of feldspar porphyry which, in turn, grade eastward into strongly flow-banded 141 Ma rhyolite lava and tuff [*Addison*, 1986]. On Harker diagrams [Figure 6, cf. *Sewell and Campbell*, 1997], these plutonic and volcanic rocks display a comagmatic fractionation trend from dominantly intermediate compositions in the west to highly silicic compositions in the east.

In southern Hong Kong Island and on Lamma Island, magmatically foliated quartz monzonite to monzogranite stocks and dikes occur as discontinuous E- to NE-trending intrusions. These can be traced eastward through the 143 Ma volcanic sequence into the basal portion of the 141 Ma volcanic sequence (Figure 2), where the monzonitic bodies are closely associated with volcanic conduit materials, including polymictic tuff breccia [*Strange et al*., 1990; Figure 5D]. Field exposures in southeast Hong Kong Island, reveal that monzonitic stocks and dikes are intruded by granite very similar in composition to the pluton centered on Kowloon. This observation is consistent with U-Pb zircon geochronology [*Davis et al*., 1997; *Sewell et al*.,

160 2012] which suggests that the granite pluton centered on Kowloon (140.4 ± 0.2 Ma) is slightly
161 younger than the monzonitic intrusions (140.6 ± 0.3 Ma). Marine boreholes and surface
162 exposures on small islands immediately west of Hong Kong Island reveal that most of the
163 offshore area to the north of Lamma Island and to the west of Hong Kong Island is underlain by
164 quartz monzonite. Quartz monzonite recovered from the boreholes displays mesocumulate
165 texture and in general, is compositionally more primitive (59–63 wt% SiO_2) than quartz
166 monzonite exposed farther east (66–68 wt% SiO_2, see Dataset DS03). On Harker diagrams
167 (Figure 6), the quartz monzonite to monzogranite stocks and dikes lie on a fractionation lineage
168 related to 141 Ma volcanic rocks exposed farther east.
169 Coeval mafic enclaves have been reported in the 141 Ma monzogranite from Lamma
170 Island [*Strange and Shaw*, 1986; *Sewell et al*., 2000; Figure 5E]. These high K, low Ti,
171 shoshonitic monzodiorite enclaves are of similar composition to mafic dikes that intrude the
172 High Island tuff in eastern New Territories [*Sewell et al*., 2000, Figure 5F].
173 **4. Early Cretaceous Tectonomagmatic Structures**
174 **4.1 Tectonomagmatic Structures Revealed by Geophysical Data**
175 Regional gravity and marine magnetic surveys carried out by the Hong Kong
176 Government [*Electronic and Geophysical Services Ltd*., 1991; *Busby et al*., 1992; *Fletcher et al*.,
177 2000; *Sewell et al*., 2000] have revealed the continuity and depth of structures that influenced
178 Early Cretaceous magmatism beneath Hong Kong. Recognition of these structures is based on
179 the coincidence of gravity and magnetic anomalies with tabular magmatic bodies, particularly
180 the monzonitic dikes.
181 Gravity models developed for Hong Kong [*Fletcher et al*., 1997] have included the
182 application of the Euler deconvolution technique [*Reid et al*., 1990] to interpret basement

183 structures. The technique provides an indication of source geometry and depth from gravity data
184 without the need for prior knowledge of structures or reference to physical properties of the
185 rocks. However, the solutions depend on sufficient density contrasts in the structures to generate
186 anomaly gradients. Euler solutions calculated from Hong Kong-wide Bouguer gravity data
187 (Figure 7A) reveal linear, arcuate, and sigmoidal anomalies. Some can be directly linked with
188 faults and caldera boundaries mapped at the surface; others are interpreted as deeper structures
189 without known surface expression [*Fletcher et al*., 1997]. Of particular interest are E- and N-
190 trending anomalies with solution depths from 1 to 8 km which are concentrated mainly in eastern
191 offshore areas (SI 1, Figure 7A). A major structural boundary is also suggested by shallow depth
192 solutions west of Lamma Island which separate dominantly linear anomalies in the north and east
193 from mainly arcuate and sigmoidal anomalies in the west and south (Figure 7A). Linear
194 anomalies that vary in length between 2 and 10 km, and are up to 500 m wide, are thought to
195 correspond to faults in the uppermost part of the middle crust and the upper crust.

196 The magnetic anomaly map [*Fletcher et al*., 2000; *Sewell et al*., 2000] for eastern and
197 southern Hong Kong waters (based on over 1000 line-kilometers of marine magnetic data
198 profiles) shows several lineaments that represent the offshore continuation of mapped faults
199 (Figure 7A). Additionally, several magnetic lineaments which align with Euler anomalies appear
200 not to have known onshore fault equivalents (e.g., N-trending structures in easternmost waters,
201 and E-trending structures near Sai Kung). Offshore quartz monzonite bodies, proven by marine
202 drilling and undersea tunnel excavation [*Fletcher et al*., 2000], generally define magnetic ridges.
203 In southwestern Hong Kong, the magnetic ridges correlate with onshore quartz monzonite
204 intrusions along faults and help to delineate caldera-related structures. A prominent E–W-

205 trending magnetic ridge immediately to the southeast of Hong Kong Island has been interpreted
206 to reflect a quartz monzonite intrusion [*Fletcher et al*., 2000].

207 Magnetic anomalies in the offshore area to the northwest of Lamma Island suggest the
208 existence of a WNW-ESE structural boundary separating magnetically neutral granitic rocks in
209 the north and east from magnetically positive granitic rocks in the south [*Fletcher et al*., 2000].
210 Magnetic ridges interpreted as quartz monzonite intrusions can be traced for 12 km
211 southwestward from west Kowloon where they appear to terminate against magnetically positive
212 granitic rocks near Lantau Island. Immediately to the west and north of Lamma Island, two
213 dipolar, extremely strong magnetic anomalies (>3000 nT) with positive values in the south and
214 negative values in the north have been interpreted as steeply plunging, highly magnetic basic
215 plugs within 250 m of the seafloor [*Fletcher et al*., 2000].

216 Field and geophysical observations have led to recognition that the structural
217 configuration in eastern and southern Hong Kong represents a combination of both depth and
218 lateral dimensions of a large collapse caldera system. Due to the prevailing dip of the strata, the
219 depth dimension is expressed largely as a lateral dimension and this explains the variable
220 orientation of caldera-bounding faults and related structures. The lateral dimension is
221 foreshortened due to the dominance of the depth dimension. Consequently, the apparent sinistral
222 and dextral offsets of caldera-bounding faults and related structures have a significant vertical
223 component related to the collapse phase of caldera development.

224 **4.2 Caldera-bounding faults and related structures**

225 Several faults are interpreted as having strongly influenced caldera development, and
226 having served as magma conduits, during the two Early Cretaceous ‘flare-ups’ [*Campbell and*

227 *Sewell*, 1997]. These include the Tolo Channel, Chek Keng, Wong Chuk, Tin Ha Shan, Jordan
228 Valley Tiu Keng Leng, and Sheung Sze Mun faults (Figure 2).

229 (a) The NE-trending Tolo Channel Fault (Figure 2) approximates the boundary between the
230 Jurassic and Cretaceous volcanic–plutonic associations (Figure 1). On the magnetic anomaly
231 map for western Victoria Harbour [*Sewell et al*., 2000], the fault marks the abrupt termination of
232 a major ENE-trending, Late Jurassic dike swarm, most extensively developed on eastern Lantau
233 island.

234 (b) The E- to ENE-trending Chek Keng Fault (Figure 2) is characterized by sporadic
235 intrusions of quartz monzonite to monzogranite and has previously been interpreted as marking
236 the E-W boundary between the Long Harbour 'caldera' and the High Island 'caldera' [*Strange et*
237 *al*., 1990; *Campbell and Sewell*, 1997, Figure 1]. Farther west, the fault displays a southwestward
238 bend and eventually coincides with monzonitic dikes which intrude granite in the central New
239 Territories. The fault marks the northern boundary of a major conduit that fed rhyolite lava
240 belonging to the 141 Ma 'flare-up', whereas in the east it is terminated abruptly by a N-trending
241 fault. The easterly-dipping 143 Ma volcanic sequences on either side of the fault have been
242 offset, apparently dextrally and probably vertically to a significant extent, by approximately 10
243 km.

244 (c) The NE-trending Wong Chuk Fault (Figure 2) was previously thought to mark the
245 northwestern boundary of the Sai Kung 'caldera' [*Sewell et al*., 2000]. It is characterized for
246 most of its 8 km length by a 100 m-wide quartz monzonite intrusion which marks the southern
247 boundary to the 141 Ma rhyolite lava conduit described above (opposite to the Chek Keng Fault).
248 In the southwest, the Wong Chuk Fault bifurcates, one segment of which continues linearly to
249 coincide with a zone of numerous NE-trending monzonitic dikes, and the other which bends to

250 the south, and then to the southwest, before terminating in the 141 Ma granite plutons centered
251 on Kowloon.

252 (d) The E- to ENE-trending Tin Ha Shan Fault (Figure 2) is characterized in eastern
253 Kowloon by a 1400 m-wide volcanic conduit infilled with block-rich pyroclastic material and
254 dikes of quartz monzonite to monzogranite. On Hong Kong Island, the fault coincides with a
255 discontinuous tabular NE-trending quartz monzonite to monzonite intrusion which passes
256 through central Hong Kong Island.

257 (e) The NE-trending Jordan Valley Fault (Figure 2) was previously thought to mark the
258 southeastern boundary of the Sai Kung 'caldera' and was inferred [*Sewell et al*., 2000] to link up
259 with sporadic monzonite intrusions farther northeast. We now consider that a WNW-trending
260 fault mapped through High Island Reservoir [*Strange et al*., 1990; *Sewell et al*., 2000], makes a
261 southwestward bend to coincide with the Jordan Valley Fault. The contact between the High
262 Island tuff and underlying rhyolite lava unit on either side of the fault has been offset, apparently
263 dextrally, by approximately 3 km, and provides compelling evidence that this fault is the
264 southeastern bounding fault of the caldera.

265 (f) The NE-trending Tiu Keng Leng Fault (Figure 2) is associated with a NE-trending quartz
266 monzonite intrusion in eastern Kowloon [*Geotechnical Control Office*, 1986, 1989a, 1989b]. In
267 Sai Kung, the fault is inferred make a right angle bend to coincide with an E-trending offshore
268 magnetic lineament (see below). The fault is responsible for apparently sinistral offsets of the
269 volcaniclastic unit and the trachydacite lava unit belonging to the 143 Ma and 141 Ma 'flare-
270 ups', respectively.

271 (g) The ENE-trending Sheung Sze Mun Fault (Figure 2) is inferred to mark the southern
272 boundary of the Early Cretaceous volcanic–plutonic association in Hong Kong. It is defined by a

strong magnetic ridge interpreted as a quartz monzonite intrusion in the offshore channel immediately to the southeast of Hong Kong Island. Granitic rocks on islands to the south of the channel have been dated as belonging to the 146 Ma 'flare-up' [*Sewell et al*., 2012].

5. Tilted Nested Caldera Complex

Available geological, geochemical and geophysical evidence show that southeastern Hong Kong, comprising mainly Early Cretaceous granitic rocks in the southwest and volcanic rocks in the northeast, and bounded by the Tolo Channel Fault in the north and the ENE-trending Sheung Sze Mun Fault in the south, has been tilted eastward by up to 30º. This has resulted in near continuous exposure for 30 km (east to west) revealing a vertical crustal section approximately 14 km thick, from the floor of the magma chamber to the top of the exposed caldera infill (Figure 7B). The caldera complex is dominated by the High Island Caldera and its comagmatic subvolcanic intrusions. These are nested within a 143 Ma volcanic–plutonic assemblage, representing an earlier caldera complex, which was strongly dismembered during the subsequent 141 Ma 'flare-up' and caldera collapse.

The southern and northern boundaries of the High Island Caldera are delimited by tabular quartz monzonite to monzogranite intrusions along faults, which fed trachydacite-rhyolite domes and volcanic conduits exposed in easternmost outcrops. The eastern boundary of the caldera is represented by N–S trending magnetic and gravity (Euler) lineaments which probably mark intrusions along faults at depth. The western boundary, exposing a deeper crustal level, is marked by NW- to N-trending mesocumulate-textured quartz monzonite to monzogranite intrusions west of Hong Kong Island. These link with quartz monzonite to monzogranite dikes from the central New Territories, and probably represent the residue of the evacuated magma chamber.

We interpret the Chek Keng, Jordan Valley and Tiu Keng Leng faults associated with monzonitic intrusions and with pronounced bends, as caldera collapse-related structures (Figure 7B). Kilometer-scale vertical subsidence is inferred along these faults on the basis of evidence from: geochemical correlation of fault-bounded volcanic blocks comprising volcanic strata of the 143 Ma flare-up; offsets of mappable contacts; and thickness variations among the 141 Ma volcanic units. The previously interpreted 143 Ma 'calderas' are now considered to belong to a single 143 Ma caldera (redefined here as the Sai Kung Caldera). A relatively intact upper crustal remnant of this caldera is preserved adjacent to the Tolo Channel Fault, along the northern margin of the nested caldera complex (Figure 7B). This reveals an eastward-dipping (up to 30º dip) layered sequence comprising the 143 Ma, 146 Ma, and 164 Ma volcanic successions. These overlie older sedimentary rocks and are intruded at depth by 143 Ma plutons. Along the southern margin of the nested caldera complex, the Sai Kung Caldera has been extensively dismembered by subsequent collapse of the High Island Caldera and intrusion of 141 Ma plutons. The strongly folded blocks of fine ash vitric tuff on Hong Kong Island, compared to the relatively intact tuff blocks in eastern Kowloon, represent massive disruption and foundering of the 143 Ma volcanic assemblage due to collapse of the subsequent High Island Caldera (Figure 7B). Asymmetric block collapse of the caldera may have promoted the deep foundering of the 143 Ma volcanic assemblage [cf. Questa Caldera, *Lipman*, 1983, see below]. Several mega-xenolithic blocks of volcanic and plutonic material belonging to the 164 Ma magmatic episode also collapsed deeply into the underlying magma chamber and are now enveloped by quartz monzonite and monzogranite intrusions on the southern margin of the caldera complex.

Caldera-bounding faults delimited by quartz monzonite to monzogranite intrusions are vestiges of the plumbing system related to the overlying High Island Caldera. They probably

served as major conduits for the evacuating 141 Ma magma chamber. Slightly more primitive, mesocumulate-textured quartz monzonite stocks in the west, compared to the east, possibly represent unerupted crystal-rich portions of the magma chamber. Coeval mafic enclaves in associated monzogranite, combined with magnetic anomalies suggesting near surface mafic intrusion, indicate involvement of mafic magma in the source. Abrupt changes in magnetic and gravity patterns in the offshore area to the west of Lamma Island probably delineate the southwestern limit of the nested caldera complex which also corresponds to its deepest level of exposure. Reconstruction of the upper crustal geometry for southeastern Hong Kong (Figure 8A) suggests that it represents a tilted cylinder-shaped nested caldera complex. This is made up of many collapsed crustal blocks. Tilting of the nested caldera complex (Figure 8B) probably occurred during, or immediately after, paroxysmal evacuation of the High Island tuff.

The 141 Ma granites centered on Kowloon most likely represent magmatic recharge of the evacuated reservoir that fed the High Island tuff. Magmatic resurgence further deformed the collapsed crustal blocks, particularly on southern Hong Kong Island. Subsequently, the Early Cretaceous nested calderas and their subvolcanic plutons were uplifted and eroded to expose the present crustal extent (Figure 8C).

6. High Island Tuff Supereruption

The compositionally uniform, densely welded, High Island tuff is considered to represent the intracaldera fill of an immense eruption that signaled the end of Mesozoic silicic volcanic activity in Hong Kong [*Strange et al*., 1990; *Campbell and Sewell*, 1997; *Sewell et al*., 2000]. A colossal volume of pyroclastic material ponded and cooled within the depression. What remains preserved is a single cooling unit of tuff with gigantic columnar joints (columns up to 2 m diameter). Outflow and co-ignimbrite ash fall deposits from this eruption have now been

completely eroded, except for an uppermost 25-m thick fine ash tuff unit (141 Ma) within the Lantau Caldera which may represent a preserved remnant of the outflow sheet. The High Island tuff is interpreted as the erupted, highly differentiated upper portion of a large, shallow, zoned quartz monzonite to high-silica granite magma body. Quartz monzonite dikes and stocks, representing tapping of the crystal-rich portion of the magma chamber, were injected into the main volcanic conduits at a late stage of the eruption. Some of these differentiated internally to monzogranitic compositions as they ascended. Sporadic mafic dikes, possibly representing a mafic underplate at depth, were intruded simultaneously with, or immediately after, the emplacement of quartz monzonites, but reached higher levels, including the basal portion of the still cooling High Island tuff. Resurgent activity, marked by the large 141 Ma granite body centered on Kowloon, probably caused further deformation of collapsed 143 Ma crustal blocks.

6.1 Eruptive Volume

Estimates of the eruptive volume of the High Island tuff are necessarily speculative owing to the virtual absence of deposits outside the known boundaries of the caldera, and uncertainties over the amount of regional erosion. However, some rough estimates are possible, even where only a remnant intracaldera fill deposit is preserved, based on knowledge of some well-studied ignimbrites and ash-flow calderas [e.g., *Wilson*, 2001; *Lipman*, 2007]. The first ingredient to establish is the average bulk density of the tuff. This can be done either by direct measurement, or by calculation on the basis of whole-rock chemistry.

The saturated bulk density of the High Island tuff, measured in accordance with the International Society for Rock Mechanics Suggested Methods [Brown, 1981], is 2560 kg m^{-3}, which is slightly higher than the range of values (2000–2500 kg m^{-3}) normally quoted for welded ignimbrites [*Mason et al*., 2004]. On the basis of whole-rock chemistry, the average bulk density

365 of the tuff is 2300 kg m^{-3} using the computer program 'KWare Magma' available from KWare-
366 Geological Software (http://geodynamics.lanl.gov/Wohletz/Magma.htm). We propose, therefore,
367 that the best estimate of the average bulk density for the High Island tuff lies midway between
368 these two end members at approximately 2430 kg m^{-3}. This is close to the average bulk density
369 (2450 kg m^{-3}) used by *Mason et al.* [2004] to compare the sizes of the largest known ignimbrite
370 deposits on Earth.

371 The minimum thickness of High Island tuff, measured from its basal contact with the
372 underlying rhyolite lava to its easternmost exposure, is about 1 km. However, fission track
373 thermochronometric data from neighbouring Guangdong Province [*Yi et al*., 2009] suggests 3–6
374 km of regional unroofing since the Late Cretaceous. So this minimum thickness of intracaldera
375 ash flow deposit may be a considerable underestimate.

376 The structural boundaries of the High Island Caldera, delineated by quartz monzonite and
377 monzogranite dike intrusions, volcanic conduits, marked angular unconformities with underlying
378 units, mesobreccias, etc, are projected to form an ellipsoid in outline with a north-south long axis
379 of c.18 km. Based on a minimum thickness of intracaldera ash flow deposit of 1 km, and a
380 caldera diameter of 18 km, the estimated dense rock equivalent (DRE) intracaldera volume of the
381 High Island tuff is ~250 km^3. *Lipman* [1984] proposed that the outflow deposit (O) volume is
382 approximately equivalent to the intracaldera ash flow deposit (I) volume. In a similar manner,
383 *Sparks and Walker* [1977] suggested that some outflow deposit volumes approximated the co-
384 ignimbrite ash fall deposit (A) volume. Assuming that the co-ignimbrite ash fall deposit for the
385 High Island eruption had an average dry bulk density of 700 kg m^{-3} (midpoint of the range (600–
386 800 kg m^{-3}) for fresh rhyolitic ash fallout [*Shipley and Sarna-Wojcicki*, 1982]), and scaling
387 against the estimated bulk density for welded ignimbrite, then the minimum volume of magma

388 erupted (I + O + A) is estimated as ~570 km^3. This falls within the general definition of a
389 supereruption [e.g., *Mason et al*., 2004].

390 **6.2 Western USA Cordillera and Southeastern China Analogs**

391 We consider that the Questa Caldera in northern New Mexico, USA, [*Lipman*, 1983;
392 *Johnson et al*., 1989] represents a close analog of the High Island Caldera in terms of
393 topographic dimensions (>15 km diameter), volume (>500 km^3) and high-SiO_2 composition (76–
394 78 wt%) of material erupted, collapse style, and the exposed volcanic–plutonic connections. The
395 26 Ma Questa Caldera developed above a shallow, quartz monzonite to granite magma body
396 undergoing extension along regional faults. The extensional tectonic setting is thought to have
397 influenced asymmetric collapse of the caldera during eruption of the Amalia Tuff, and intense
398 deformation and rotation of foundering crustal blocks. A shallow granite body is also thought to
399 represent a resurgent intrusion within the caldera.

400 Similarly, though on a smaller scale, we consider that the Searchlight pluton in the
401 Eldorado Mountains, Nevada, USA, [*Bachl et al*., 2001] represents a compositional and
402 structural analog of the subvolcanic magma chamber that fed the High Island tuff.
403 Reconstruction of the Searchlight pluton from an interpreted tilted crustal section has unveiled a
404 fossil magma chamber. This comprises a lower basal unit of magmatically foliated quartz
405 monzonite containing synplutonic mafic pods, a middle unit of granite, and an upper roof unit of
406 quartz monzonite. The lower and middle units are considered to represent the segregated melt-
407 rich and crystal-rich portions, respectively, of a solidifying magma body; the upper unit is
408 thought to represent a solidification front. Synplutonic mafic pods have been interpreted as
409 indicating injections of variably contaminated mantle-derived magma in the source region.

Several large volcanic–plutonic complexes have been described from the Mesozoic Yanshanian magmatic belt of southeastern China, mainly in western Guangdong [*Geng et al*., 2006], Fujian [*Qiu et al*., 1999] and Jiangxi [*Yang et al*., 2011] provinces. However, most of these studies have focused on petrological and geochemical aspects, and relatively few details are readily available on pluton-caldera dimensions, subvolcanic structural connections, and volumes of erupted materials. Nevertheless, the increasing application of high precision U-Pb zircon geochronology to studies of such complexes has revealed the potential for close analogies with Hong Kong. For example, the Early Cretaceous Xiangshan volcanic–plutonic complex in Jiangxi Province [*Yang et al*., 2011] comprises an early stage of fissure-fed dacite to rhyolitic welded ignimbrite eruption, with associated monzogranite porphyry, and a late stage, central vent caldera-forming eruption of rhyolite tuff, with associated injection of quartz monzonite and high-K mafic dikes. Interestingly, the U-Pb zircon ages reveal that the emplacement of the Xiangshan magmatic complex took place over approximately two million years, which is of similar duration to the Early Cretaceous 'flare-ups' in Hong Kong.

7. Conclusion

The exceptional detail afforded by this remarkable crustal section through a nested caldera complex in southeastern Hong Kong provides a direct window into the magmatic and tectonic origins of large, overlapping, silicic magmatic systems. Reconstruction of the geometry of the nested caldera complex, based on meticulous field observations, high precision geochronology, whole-rock geochemistry, and geophysical surveys, reveals that the 143 Ma volcanic–plutonic assemblage was extensively dismembered by development of the spatially overlapping 141 Ma High Island Caldera. Rapid evacuation of a large, shallow, silicic magma chamber during the 141 Ma 'flare-up' possibly induced asymmetric collapse of the nested

caldera complex to produce a local NE-oriented tilted crustal section. Volcanic conduits from which immense 141 Ma eruptions took place were concentrated mainly along caldera ring fault zones, some of which permitted the collapse of kilometer-scale crustal blocks to abyssal depths of the underlying magma chamber. These are now preserved either as composite (quartz monzonite to monzogranite) feeder dike complexes, or as quartz monzonite and monzogranite stocks. The volcanic conduits, and the structures within which they occur, therefore reveal a direct connection between the magma chamber and the extrusive rocks. They were exploited repeatedly during the 141 Ma 'flare-up', from the early stage extrusion of trachydacite to rhyolite lavas and tuffs, through the main stage eruption of the High Island tuff, to the late extrusion of less differentiated magma. The rapid accumulation, ponding, and uniform cooling of the intracaldera High Island tuff resulted in the development of the spectacular columnar-jointed rhyolitic rock masses. Many of the features of the tilted nested caldera complex warrant further examination, the details of which are beyond the scope of this paper. However, it is hoped that future studies will provide valuable new insights into magma assemblies, eruption mechanisms, and structural development of large silicic magmatic systems.

The nested caldera complex in southeastern Hong Kong is considered to represent an exemplar of similar Middle Jurassic to Early Cretaceous magmatic systems that were replicated many times during ignimbrite 'flare-ups' over 100,000's of square kilometers along the southeastern seaboard of China. We consider that the Early Yanshanian magmatic belt in southeastern China culminated in a surge of pulsed supereruption scale magmatic activities straddling the Jurassic–Cretaceous boundary and ended abruptly at approximately 141 Ma. The ignimbrite 'flare-ups' recognized in Hong Kong represent a microcosm of these activities. Such voluminous ignimbrite 'flare-ups' coinciding with the end of the Early Yanshanian magmatic

period would have had global environmental impact and may have influenced the widespread extinction event among marine tetrapod and terrestrial dinosaur faunas at the end-Jurassic [*Bakker*, 1978; *Barrett et al.,* 2009; *Benson et al*., 2009].

Acknowledgments

We are grateful to Jim Cole and Mike Branney for helpful comments on early drafts of the manuscript, and to Cheng-Hong Chen, Calvin Miller and an anonymous referee for careful reviews. This paper is published with the approval of the Director of Civil Engineering and Development and Head of the Geotechnical Engineering Office, Hong Kong SAR Government. S.D.G Campbell publishes with the permission of the Executive Director of the British Geological Survey.

References

Addison, R. (1986), Geology of Sha Tin*, Hong Kong Geological Survey Geological Memoir No. 1*, Geotechnical Control Office, Hong Kong.

Bachl, C. A., C. F. Miller, J. S. Miller and J. E. Faulds (2001), Construction of a pluton: Evidence from an exposed cross section of the Searchlight pluton, Eldorado Mountains, Nevada, *Geol. Soc. Amer. Bull.*, *113*, 1213–1228, doi:10.1130/0016-7606(2001)113<1213:COAPEF>2.0.CO;2

Bachmann, O., C.F. Miller and S.L. de Silva (2007), The volcanic–plutonic connection as a stage for understanding crustal magmatism, *J. Volcanol. Geotherm. Res., 167*, 1–23, doi:10.1016/j.jvolgeores.2007.08.002

Bakker, R.T. (1978), Dinosaur feeding behaviour and the origin of flowering plants. *Nature 274*, 661–663, doi:10.1038/274661a0.

478 Barrett, P.M., A.J. McGowan and V. Page (2009), Dinosaur diversity and the rock record. *Proc.*
479 *R. Soc. Series B, 276*, 2667–2674, doi:10.1098/rspb.2009.0352.
480 Benson, R.B.J., R.J. Butler, J. Lindgren and A.S. Smith (2009), Mesozoic marine tetrapod
481 diversity: mass extinctions and temporal heterogeneity in geological megabiases affecting
482 vertebrates, *Proc. R. Soc. Series B, 277*, 829–834, doi:10.1098/rspb.2009.1845.
483 Brown, E.T. (Ed.) (1981), *Rock Characterization Testing and Monitoring ISRM Suggested*
484 *Methods*, Commission on Testing Methods International Society for Rock Mechanics,
485 Oxford.
486 Busby, J. P., R. B. Evans, M. S. Lam, W. N. Ridley Thomas and R. L. Langford (1992), The
487 gravity base station network and regional gravity survey of Hong Kong, *Geol. Soc. Hong*
488 *Kong Newsl.*, *10*, 2–5.
489 Campbell, S. D. G. and R. J. Sewell (1997), Structural control and tectonic setting of Mesozoic
490 volcanism in Hong Kong, *J. Geol. Soc. Lond.*, *154*, 1039–1052, doi:
491 10.1144/gsjgs.154.6.1039.
492 Campbell, S. D. G., R. J. Sewell, D. W. Davis and A. C. T. So (2007), New U-Pb age and
493 geochemical constraints on the stratigraphy and distribution of the Lantau Volcanic Group,
494 Hong Kong, *J. Asian Earth Sci.*, *31*, 139–152, doi:10.1016/j.jseaes.2007.05.001.
495 Christiansen, R. L., J. B. Lowenstern, R. B. Smith, H. Heasler, L. A. Morgan, M. Nathenson, L.
496 G. Mastin, L. J. P. Muffler and J. E. Robinson (2007), Preliminary assessment of volcanic
497 and hydrothermal hazards in Yellowstone National Park and vicinity, *Open-file Report*
498 *2007–1071*, USGS, Reston, Virginia.

499 Coleman, D.S., W. Gray and A.F. Glazner (2004), Rethinking the emplacement and evolution of
500 zoned plutons: Geochronologic evidence for incremental assembly of the Tuolumne
501 Intrusive Suite, California, *Geology, 32*, 433–436, doi:10.1130/G20220.1
502 Davidson, J. P., D. J. Morgan, B. L. A. Charlier, R. Harou and J. M. Hora (2007), Microsampling
503 and isotopic analysis of igneous rocks: Implications for the study of magmatic systems,
504 *Annu. Rev. Earth Planet. Sci.*, *35*, 273–311, doi:10.1146/annurev.earth.35.031306.140211.
505 Davis, D. W., R. J. Sewell and S. D. G. Campbell (1997), U-Pb dating of Mesozoic igneous rocks
506 from Hong Kong, *J. Geol. Soc. Lond.*, *154*, 1067–1076, doi:10.1144/gsjgs.154.6.1067.
507 Electronic and Geophysical Services Ltd. (1991), Regional gravity survey of Hong Kong, *Final*
508 *Report Job Number HK50190*, Electronic and Geophysical Services Ltd., Hong Kong.
509 Fletcher, C. J. N., S. D. G. Campbell, J. P. Busby, R. M. Carruthers and K. W. Lai (1997),
510 Regional tectonic setting of Hong Kong: implications of new gravity models, *J. Geol. Soc.*
511 *Lond.*, *154*,1021–1030, doi:10.1144/gsjgs.154.6.1021.
512 Fletcher, C. J. N., F. A. Collar and M. W. C. Lai (2000), Magnetic survey of the offshore areas of
513 Hong Kong: Results, interpretation and significance, in *The Urban Geology of Hong Kong,*
514 *Geol. Soc. Hong Kong Bull. No. 6*, edited by A. Page and S.J. Reels, pp. 179-187,
515 Geological Society of Hong Kong, Hong Kong.
516 Geng, H.Y., X.S. Xu, S.Y. O'Reilly, M. Zhao and T. Sun (2006), Cretaceous volcanic-intrusive
517 magmatism in western Guangdong and its geological significance, *Sci. China Ser. D, Earth*
518 *Sci., 49*, 696–713, doi:10.1007/s11430-006-0696-7.
519 Geotechnical Control Office (1986), Hong Kong and Kowloon. *Hong Kong Geological Survey*
520 *Sheet 11, Solid and Superficial Geology, 1:20,000 Series HCM20*, Hong Kong Government,
521 Hong Kong.

Geotechnical Control Office (1989a), Sai Kung. *Hong Kong Geological Survey Sheet 8, Solid and Superficial Geology, 1:20,000 Series HGM20*, Hong Kong Government, Hong Kong.

Geotechnical Control Office (1989b), Clear Water Bay. *Hong Kong Geological Survey Sheet 12, Solid and Superficial Geology, 1:20,000 Series HGM20*, Hong Kong Government, Hong Kong.

Glazner, A.F., J.M. Bartley, D.S. Coleman, E. Gray and R.Z. Taylor (2004), Are plutons assembled over millions of years by amalgamation from small magma chambers?, *GSA Today, 14*, 4–11, doi:10.1130/1052-5173(2004)014<0004:APAOMO>2.0CO;2

Gray, W., A.F. Glazner, D.S. Coleman and J.M. Bartley (2008), Long-term geochemical variability of the Late Cretaceous Tuolumne Intrusive Suite, central Sierra Nevada, California, in *Dynamics of Crustal Magma Transfer, Storage and Differentiation*, Geol. Soc. Lond. Spec. Pub. vol. 304, edited by C. Annen and G.F. Zellmer, pp. 183–201, doi:10.1144/SP304.10.

John, D.A., C.D. Henry and J.P. Colgan (2008), Magmatic and tectonic evolution of the Caetano caldera, north-central Nevada: A tilted, mid-Tertiary eruptive center and source of the Caetano Tuff, *Geosphere, 4, 75–106*, doi:10.1130/GES00116.1

Johnson, C. M., J. R. Shannon and C. J. Fridrich (1989), Roots of ignimbrite calderas: Batholithic plutonism, volcanism, and mineralization in the Southern Rocky Mountains, Colorado and New Mexico, in *Field Excursions to Volcanic Terrains in the Western United States, Volume I: Southern Rocky Mountain Region*, Memoir 46, edited by C.E. Chapin and J. Zidek, pp. 275–302, New Mex. Bur. Min. Miner. Res., Socorro, New Mexico.

Kennedy, B. and J. Stix (2007), Magmatic processes associated with caldera collapse at Ossipee ring dyke, New Hampshire, *Geol. Soc. Amer. Bull.*, *119*, 3–17, doi:10.1130/B25980.1

Kokelaar, B. P. and I. D. Moore (2006), *Classic Areas of British Geology: Glencoe Caldera Volcano, Scotland*, British Geological Survey, Keyworth.

Li, Z. X. and X. H. Li (2007), Formation of the 1300-km-wide intracontinental orogen and postorogenic magmatic province in Mesozoic South China: A flat-slab subduction model, *Geology*, *35*, 179–182, doi:10.1130/G23193A.1.

Lipman, P.W. (1983), The Questa caldera, northern New Mexico-relation to batholiths emplacement and associated molybdenum mineralization, in *Genesis of Rocky Mountain Ore Deposits: Changes With Time and Tectonics, Proceedings*, Denver Region Exploration Geologists Society, pp. 133–149, Golden, Colorado.

Lipman, P. W. (1984), The roots of ash-flow calderas in western North America: windows into the tops of granitic batholiths, *J. Geophys. Res.*, *89*, 8801–8841, doi: 10.1029/JB089iB10p08801.

Lipman, P.W. (2007), Incremental assembly and prolonged consolidation of Cordilleran magma chambers: Evidence from the Southern Rocky Mountain volcanic field, *Geosphere*, *3*, 42–70, doi:10.1130/ges00061.1.

Mason, B. G., D. M. Pyle and C. Oppenheimer (2004), The size and frequency of the largest explosive eruptions on Earth, *Bull. Volcanol.*, *66*, 755–748, doi:10.1007/s00445-004-0355-9.

Qiu, J.S., D. Wang and J.C. Zhou (1999), Geochemistry and petrogenesis of the late Mesozoic bimodal volcanic rocks at Yunshan caldera, Yongtai County, Fujian Province, *Acta Petrol. Mineral. 18,* 97–107 [in Chinese].

566 Quick, J. E., S. Sinigoi, G. Peressini, G. Demarchi, J. L. Wooden and A. Sbisa (2009), Magmatic
567 plumbing of a large Permian caldera exposed to a depth of 25 km, *Geology*, *37*, 603–606,
568 doi:10.1130/G30003A.1.
569 Reid, A. B., J. M. Allsop, H. Granser, A. J. Milletand and I. W. Somerton (1990), Magnetic
570 interpretation in three dimensions using Euler deconvolution, *Geophysics*, *55*, 80–91,
571 doi:10.1130/G30003A.1.
572 Reid, M.R., J.A. Vazquez and A.K. Schmitt (2011), Zircon-scale insights into the history of a
573 Supervolcano, Bishop Tuff, Long Valley, California, with implications for the Ti-in-zircon
574 geothermometer, *Contrib. Mineral. Petrol., 161*, 293–311, doi:10.1007/s00410-010-0532-0.
575 Sewell, R. J. and S. D. G. Campbell (1997), Geochemistry of coeval Mesozoic plutonic and
576 volcanic suites in Hong Kong, *J. Geol. Soc. Lond.*, *154*,1053–1066,
577 doi:10.1144/gsjgs.154.6.1053.
578 Sewell, R. J., D. P. F. Darbyshire, R. L. Langford and P. J. Strange (1992), Geochemistry and Rb–
579 Sr geochronology of Mesozoic granites from Hong Kong, *Trans. Roy. Soc. Edin. Earth*
580 *Sci.*, *83*, 269–280.
581 Sewell, R. J., S. D. G. Campbell, C. J. N. Fletcher, K. W. Lai and P. A. Kirk (2000), *The Pre-*
582 *Quaternary Geology of Hong Kong*, Geotechnical Engineering Office, The Government of
583 the Hong Kong Special Administrative Region, Hong Kong.
584 Sewell, R. J., D. W. Davis and S. D. G. Campbell (2012), High precision U-Pb zircon ages for
585 Mesozoic igneous rocks from Hong Kong. *J. Asian Earth Sci.*, *43,* 164–175,
586 doi:10.1016/j.jseas.2011.09.007.
587 Shipley, S. and A.M. Sarna-Wojcicki (1982), Distribution, thickness, and mass of Late
588 Pleistocene and Holocene tephra from major volcanoes in the northwestern United States: a

preliminary assessment of hazards from volcanic ejecta to Nuclear reactors in the Pacific Northwest, *USGS Misc. Field Stud. Map* MF-1435.

Sparks, R. S. J. and G. P. L. Walker (1977), The significance of vitric-enriched air-fall ashes associated with crystal-enriched ignimbrites, *J. Volcanol. Geotherm. Res.*, *2*, 329–341, doi:10.1016/0377-0273(77)90019-1 .

Strange, P. J. and R. Shaw (1986), Geology of Hong Kong Island and Kowloon*, HKGS Mem. No. 2*, Geotechnical Control Office, Hong Kong.

Strange, P. J., R. Shaw and R. Addison (1990), Geology of Sai Kung and Clear Water Bay, *HKGS Mem. No. 4*, Geotechnical Control Office, Hong Kong.

Tam S. W. and Y. M. Chan (1983), Late Jurassic ash-flow tuffs in the eastern part of Hong Kong, South China, *Asian Geographer*, *2*, 47–68.

Wilson, C.J.N. (2001), The 26.5 ka Oruanui eruption, New Zealand: an introduction and overview, *J. Volcanol. Geotherm. Res.*, *112*, 133–374, doi:10.1016/S0377-0273(01)00239-6

Yang, S.Y., S.Y. Jiang, Y.H. Jiang, K.D. Zhao and H.H. Fan (2011), Geochemical, zircon U-Pb dating and Sr-Nd-Hf isotopic constraints on the age and petrogenesis of an early Cretaceous volcanic–intrusive complex at Xiangshan, southeast China, *Miner. Petrol. 101*, 21–48, doi:10.1007/s00710-010-0136-4.

Yi Y., A. Carter, X. Bin, G. Lin, S. Brichau and X. Q. Hu (2009), A fission track and (U-Th)/He thermochronometric study of the northern margin of the South China Sea: An example of a complex passive margin, *Tectonophysics*, *474*, 584–594, doi:10.1016/j.tecto.2009.04.030.

FIGURE CAPTIONS

Figure 1. Distribution of Middle Jurassic–Early Cretaceous volcanic–plutonic associations and location of key tectonomagmatic elements in Hong Kong (after Campbell and Sewell, 1997).

612 Figure 2. Geology of southeastern Hong Kong. HIT – High Island tuff, RHY – Rhyolite lava, T-
613 VT – Trachytic subgroup - welded fine ash Vitric Tuff, T-CVT – Trachytic subgroup - Crystal-
614 bearing fine ash Vitric Tuff, R-CAT-D – Rhyolitic subgroup - Dacitic Coarse Ash crystal Tuff,
615 R-CAT-R – Rhyolitic subgroup - Rhyolitic Coarse Ash crystal Tuff, G – Granite, M – Quartz
616 Monzonite (see also Figure 4).
617 Figure 3. A: TiO_2 versus Zr plot for the 143 Ma volcanic assemblages. T-VT – Trachytic subgroup
618 - welded fine ash Vitric Tuff, T-CVT – Trachytic subgroup - Crystal-bearing fine ash Vitric Tuff,
619 R-CAT – Rhyolitic subgroup. B: TiO_2 versus Zr plot for the 141 Ma volcanic assemblages. HIT –
620 High Island tuff, RHY – Rhyolite lava. (Geochemical data used for plots are listed in data sets
621 DS01 and DS02)[1].
622 Figure 4. Composite stratigraphic column for Early Cretaceous nested volcanic centers.
623 Figure 5. Illustrations of field and rock characteristics. A) Thin section photomicrograph of densely
624 welded, High Island tuff [after *Strange et al*., 1990], B) Columnar-jointed welded High Island tuff
625 exposed on North Ninepin Island, eastern New Territories, C) Base of the High Island tuff resting
626 on tuff breccia, South Ninepin Island, eastern New Territories, D) Polymictic tuff breccia
627 representing volcanic conduit material exposed at Sai Kung, eastern New Territories, E) Coeval
628 mafic enclave displaying typical cuspate terminations in 141 Ma granite, northern Lamma Island,
629 F) Mafic dike injected along kink-band in columnar-jointed High Island tuff at High Island
630 Reservoir Dam, eastern New Territories. .
631 Figure 6. Selected Harker diagrams to illustrate comagmatic relationships between plutonic rocks
632 (quartz monzonites and monzogranites) and volcanic rocks for the 141 Ma 'flare-up'. RHY –

[1] Auxiliary Materials are available at ftp://ftp.agu.org/apend/gc/2011gc003865

633 Rhyolite lava; HIT – High Island tuff; GT/MZ – Granite/Monzonite dikes. (Geochemical data used
634 for plots are listed in data set DS03).
635 Figure 7. A: Combined offshore magnetic map, Euler gravity anomalies, major faults and magnetic
636 lineaments (after Fletcher et al., 1997; Sewell et al., 2000). B: Geologic map of the tilted nested
637 caldera-complex showing locations of key stratigraphic units, major faults and tectonomagmatic
638 boundary elements (see Figure 2 for key to abbreviations).
639 Figure 8. Block diagrams illustrating structural evolution of the tilted Early Cretaceous nested
640 caldera complex in southeastern Hong Kong (T – Trachytic subgroup, R – Rhyolitic subgroup, see
641 Figure 2 for key to other abbreviations). A: Shortly after High Island tuff eruption. B: Subsequent
642 crustal tilting by ~30 degrees. C: Uplift and erosion to reveal present-day section.
643

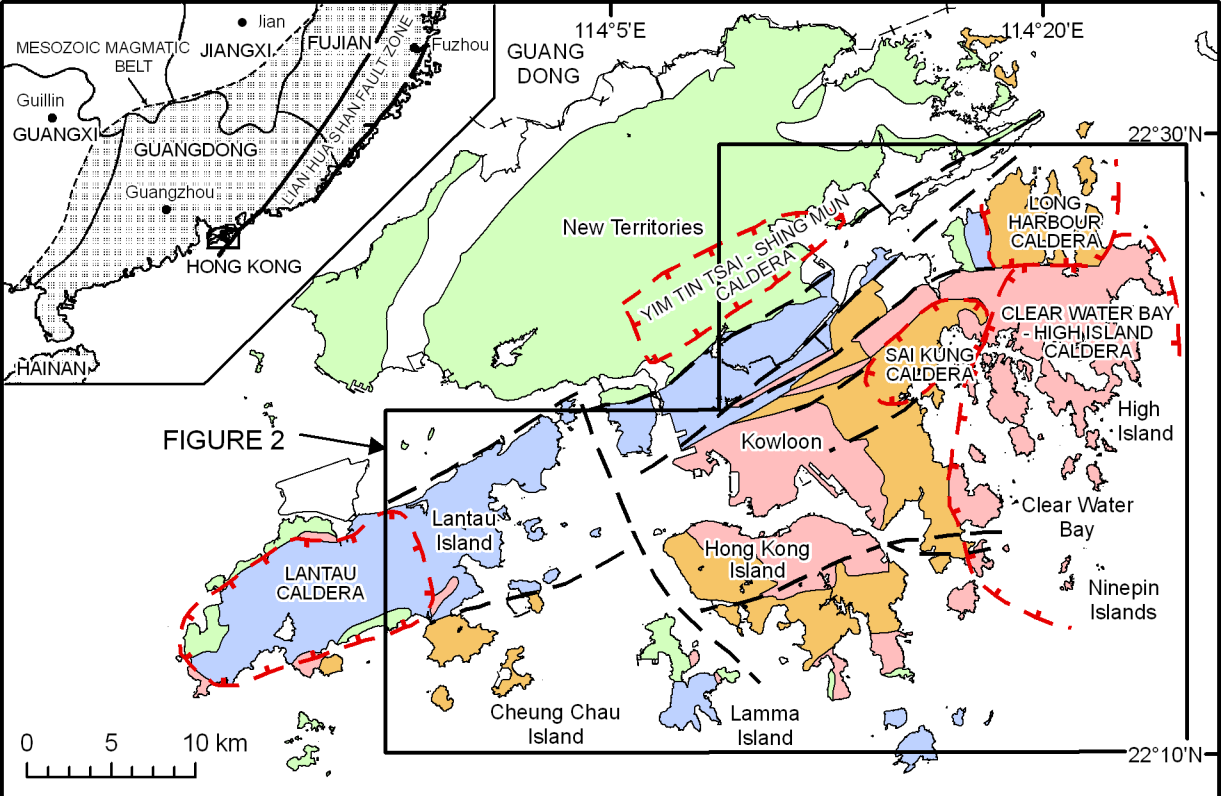

Legend

- Other rocks/sediments
- 141 Ma volcanic-plutonic rocks
- 143 Ma volcanic-plutonic rocks
- 148-146 Ma volcanic-plutonic rocks
- 164-160 Ma volcanic-plutonic rocks
- Faults/Tectono-magmatic structures
- Volcanic centers (after Campbell and Sewell, 1997)

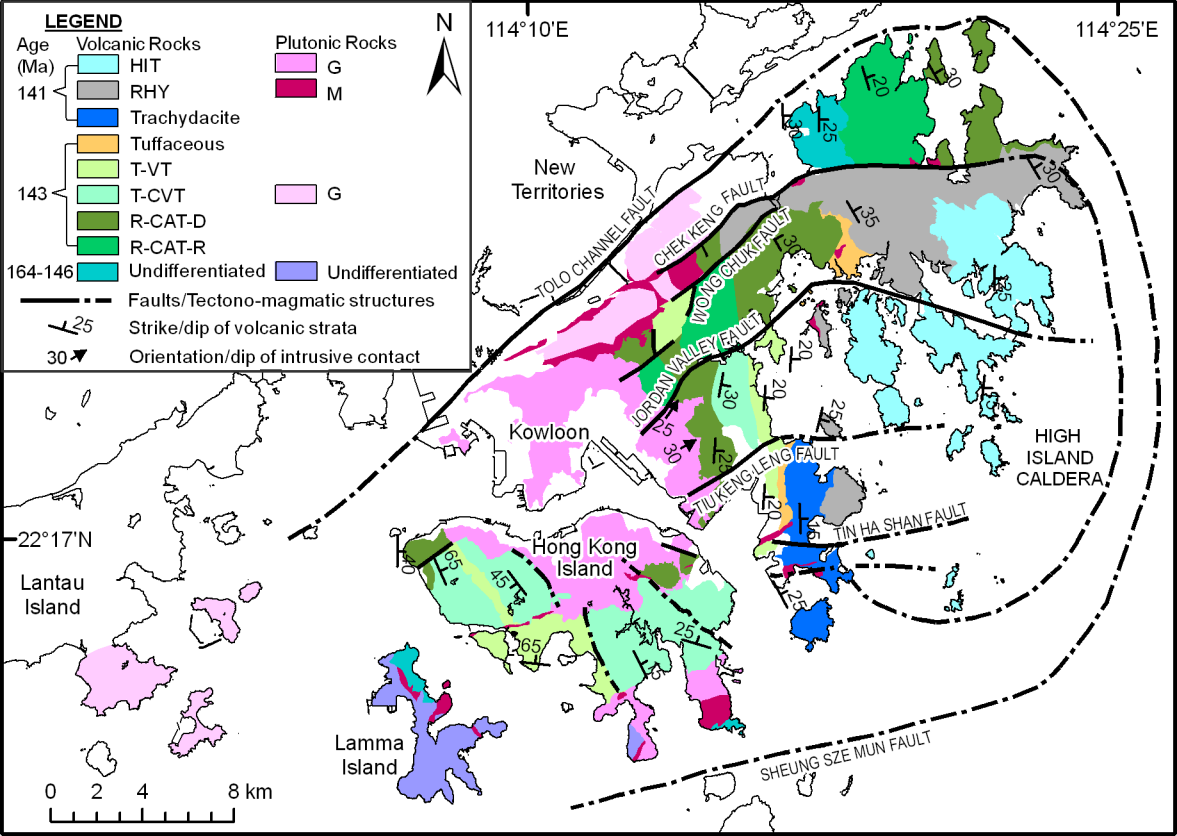
LEGEND
Age (Ma)
Volcanic Rocks
HIT
RHY
Trachydacite
Tuffaceous
T-VT
T-CVT
R-CAT-D
R-CAT-R
Undifferentiated
141
143
164-146
Plutonic Rocks
G
M
G
Undifferentiated
Faults/Tectono-magmatic structures
25 Strike/dip of volcanic strata
30 Orientation/dip of intrusive contact
N
114°10'E
114°25'E
22°17'N
New Territories
TOLO CHANNEL FAULT
CHEK KENG FAULT
WONG CHUK FAULT
JORDAN VALLEY FAULT
TIU KENG LENG FAULT
IN HA SHAN FAULT
SHEUNG SZE MUN FAULT
Kowloon
Hong Kong Island
Lantau Island
Lamma Island
HIGH ISLAND CALDERA
0 2 4 8 km

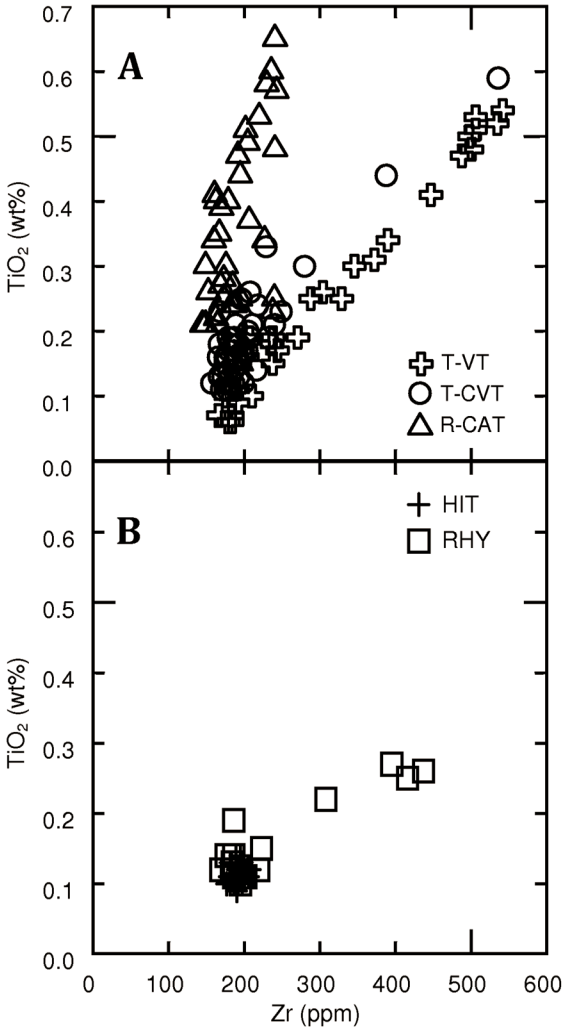
A
B
T-VT
T-CVT
R-CAT
HIT
RHY
TiO2 (wt%)
TiO2 (wt%)
Zr (ppm)
0.0
0.1
0.2
0.3
0.4
0.5
0.6
0.7
0
100
200
300
400
500
600

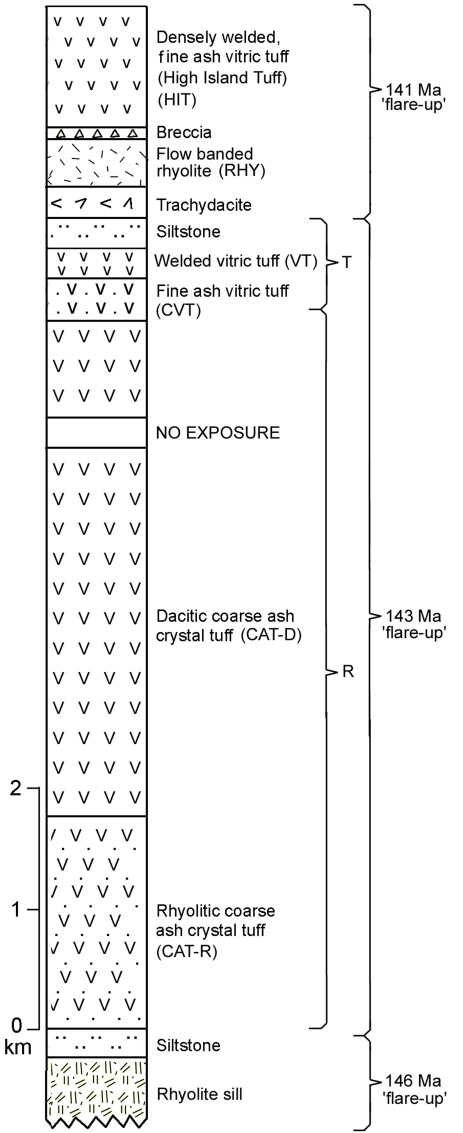
Densely welded, fine ash vitric tuff (High Island Tuff) (HIT)
Breccia
Flow banded rhyolite (RHY)
Trachydacite
Siltstone
Welded vitric tuff (VT)
Fine ash vitric tuff (CVT)
NO EXPOSURE
Dacitic coarse ash crystal tuff (CAT-D)
Rhyolitic coarse ash crystal tuff (CAT-R)
Siltstone
Rhyolite sill
141 Ma 'flare-up'
143 Ma 'flare-up'
146 Ma 'flare-up'
T
R
2
1
0
km

A
2mm

B

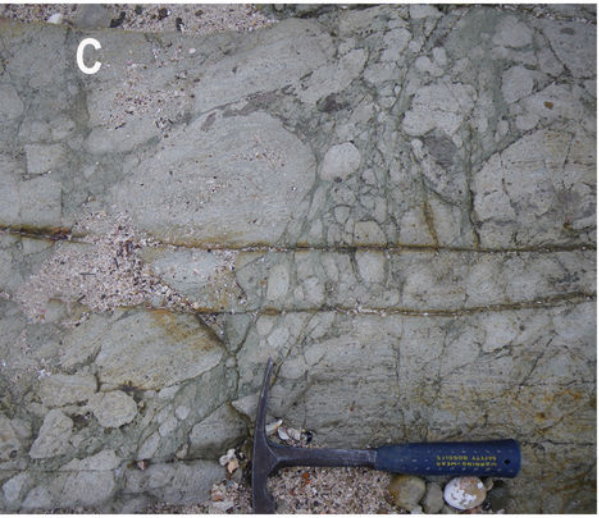
C

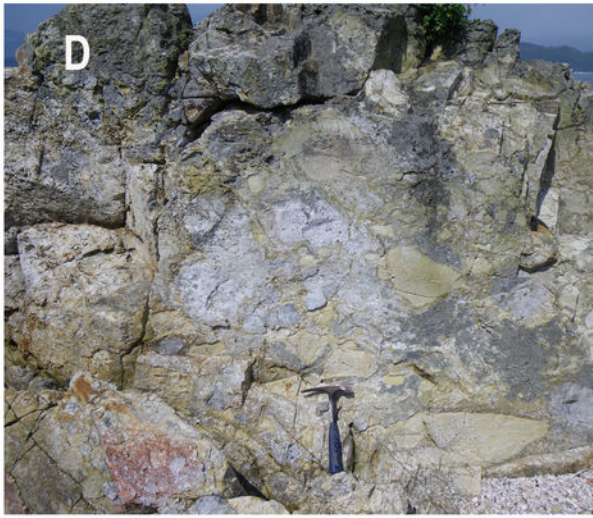
D

E

F

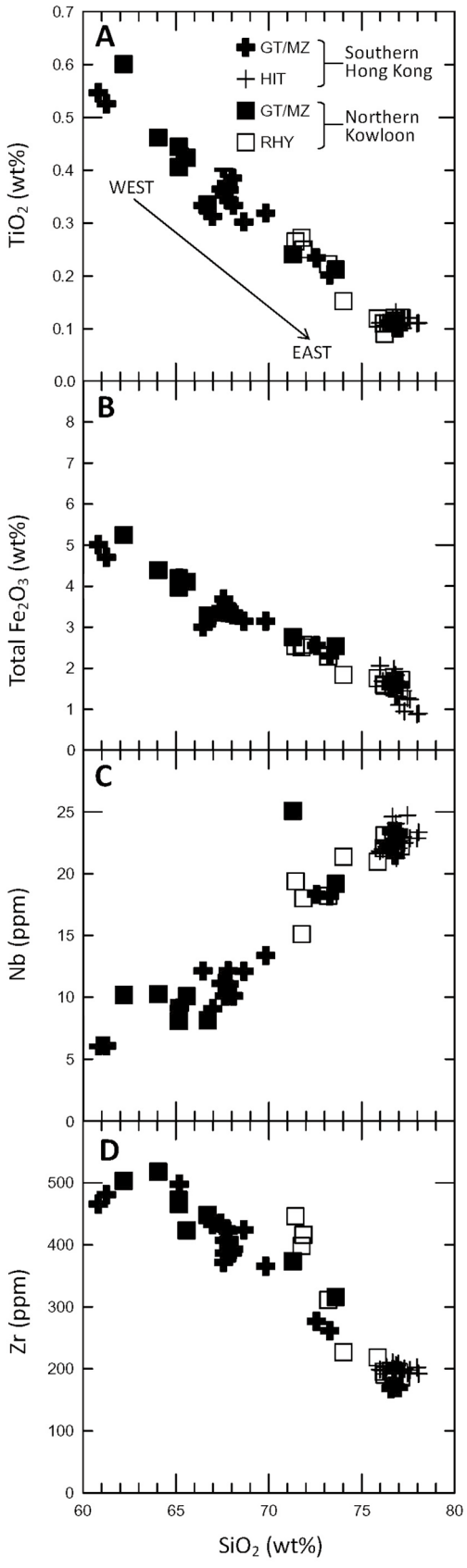
A
B
C
D
GT/MZ
HIT
Southern Hong Kong
GT/MZ
RHY
Northern Kowloon
WEST
EAST
TiO2 (wt%)
Total Fe2O3 (wt%)
Nb (ppm)
Zr (ppm)
SiO2 (wt%)

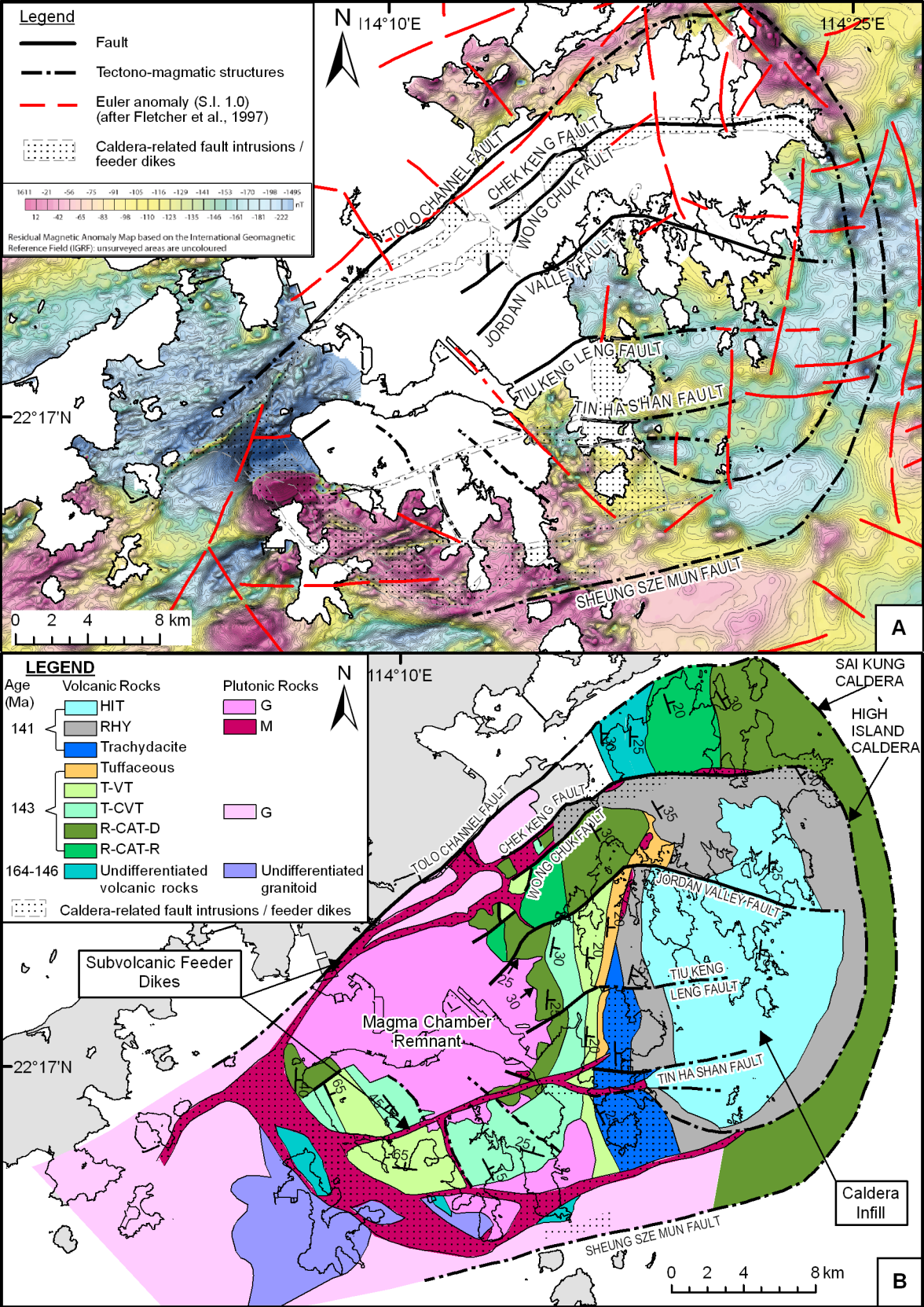
Legend
Fault
Tectono-magmatic structures
Euler anomaly (S.I. 1.0)
(after Fletcher et al., 1997)
Caldera-related fault intrusions / feeder dikes
1611 -21 -56 -75 -91 -105 -116 -129 -141 -153 -170 -198 -1495
12 -42 -65 -83 -98 -110 -123 -135 -146 -161 -181 -222
nT
Residual Magnetic Anomaly Map based on the International Geomagnetic Reference Field (IGRF); unsurveyed areas are uncoloured
N
114°10'E
114°25'E
22°17'N
TOLO CHANNEL FAULT
CHEK KENG FAULT
WONG CHUK FAULT
JORDAN VALLEY FAULT
TIU KENG LENG FAULT
TIN HA SHAN FAULT
SHEUNG SZE MUN FAULT
0 2 4 8 km
A
LEGEND
Age (Ma)
Volcanic Rocks
Plutonic Rocks
141
HIT
RHY
Trachydacite
G
M
143
Tuffaceous
T-VT
T-CVT
R-CAT-D
R-CAT-R
G
164-146
Undifferentiated volcanic rocks
Undifferentiated granitoid
Caldera-related fault intrusions / feeder dikes
SAI KUNG CALDERA
HIGH ISLAND CALDERA
Subvolcanic Feeder Dikes
Magma Chamber Remnant
Caldera Infill
0 2 4 8 km
B

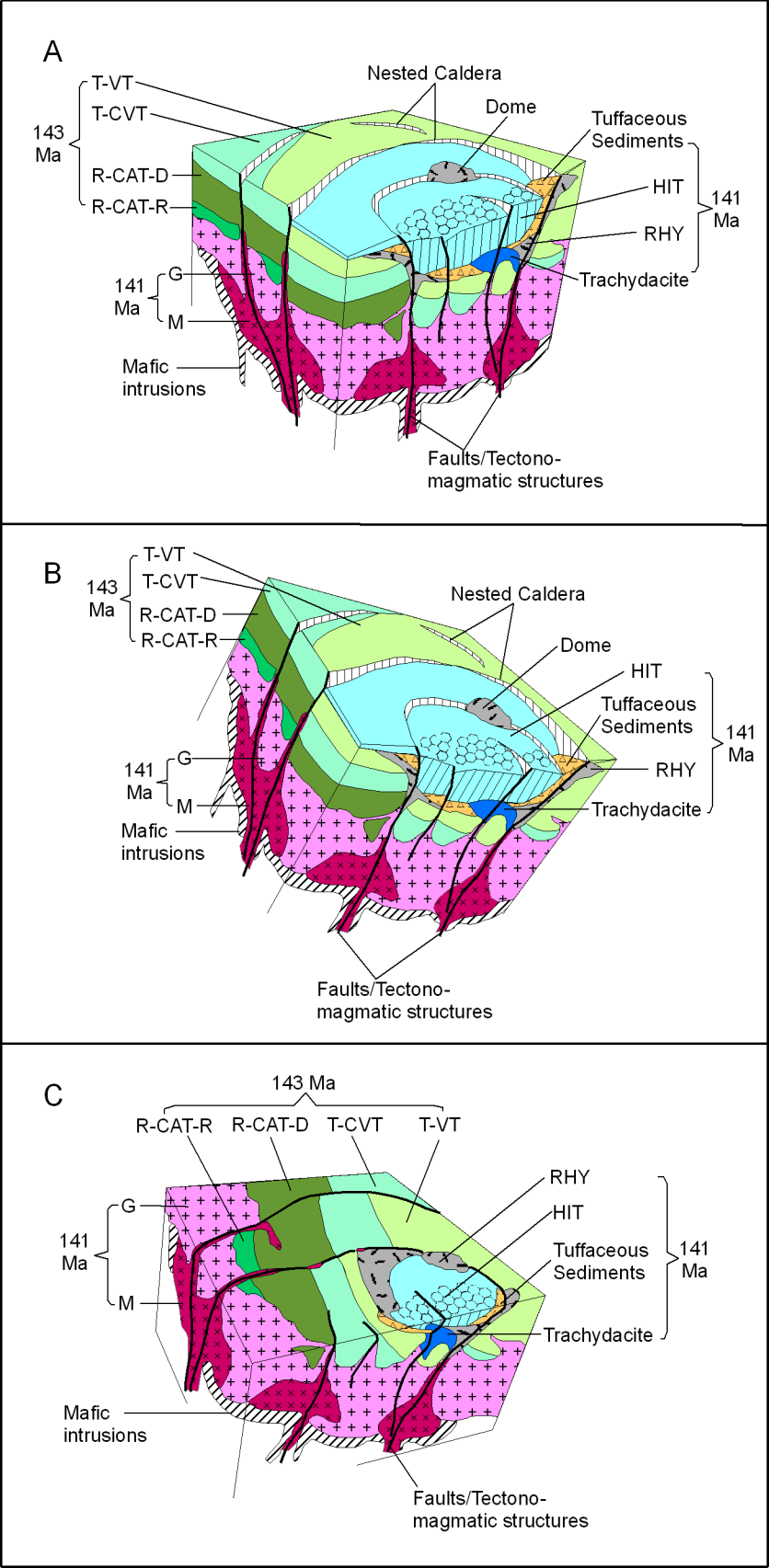
A
T-VT
T-CVT
143 Ma
R-CAT-D
R-CAT-R
Nested Caldera
Dome
Tuffaceous Sediments
HIT
RHY
Trachydacite
141 Ma
141 Ma
G
M
Mafic intrusions
Faults/Tectono-magmatic structures
B
T-VT
T-CVT
143 Ma
R-CAT-D
R-CAT-R
Nested Caldera
Dome
HIT
Tuffaceous Sediments
RHY
Trachydacite
141 Ma
141 Ma
G
M
Mafic intrusions
Faults/Tectono-magmatic structures
C
143 Ma
R-CAT-R
R-CAT-D
T-CVT
T-VT
RHY
HIT
Tuffaceous Sediments
Trachydacite
141 Ma
141 Ma
G
M
Mafic intrusions
Faults/Tectono-magmatic structures

Table 1. Summary of Middle Jurassic to Early Cretaceous Volcanic–Plutonic Associations in Hong Kong [after *Sewell et al*., 2000].

Magmatic Episode	Volcanic Group		Granitic Suite		Age[a] (Ma)
	Name	Main distribution	Name	Main distribution	
1	Tsuen Wan Volcanic Group (TWVG)	NE and NW New Territories	Lamma Suite (LS) - A-type Subsuite - I-type Subsuite	Central and W New Territories, Lamma and Lantau	165-160
2	Lantau Volcanic Group (LVG)	Central and W Lantau	Kwai Chung Suite (KCS)	E Lantau and S New Territories	148-146
3	Repulse Bay Volcanic Group (RBVG) - Rhyolitic Subgroup (R) - Trachytic Subgroup (T)	S Hong Kong, N Kowloon and Sai Kung	Cheung Chau Suite (CCS)	W Lantau and S New Territories	143
4	Kau Sai Chau Volcanic Group (KSCVG)	E New Territories	Lion Rock Suite (LRS) - Granite Subsuite (G) - Quartz Monzonite Subsuite (M)	N Hong Kong, Kowloon and E Lamma	141

[a]Based on high precision U-Pb zircon ages [*Davis et al*., 1997; *Campbell et al*., 2007; *Sewell et al*., 2012].

Table 2. General Petrologic Characteristics of Early Cretaceous Volcanic and Plutonic Rocks of Hong Kong [after *Sewell et al*., 2000].

	Repulse Bay Volcanic Group (143 Ma)		Kau Sai Chau Volcanic Group (141 Ma)	
	Rhyolitic Subgroup	Trachytic Subgroup	Clear Water Bay 'lavas and tuffs'	High Island tuff
Colour	Light grey to pinkish grey	Pale grey to bluish grey	Bluish grey to black	Pinkish grey
Texture	Coarse ash crystal tuff	Crystal-bearing fine ash vitric tuff	Porphyritic lava and fine ash vitric tuff	Crystal-bearing fine ash vitric tuff
Composition	Dacite to rhyolite (66–75 wt% SiO_2)	Trachydacite to high-silica rhyolite (63–77 wt% SiO_2)	Trachydacite to high-silica rhyolite (64–77 wt% SiO_2)	High-silica rhyolite (>75 wt% SiO_2)
Phenocrysts	Albite, oligoclase, microperthite, quartz, biotite (c.50%)	Quartz, oligoclase, albite, microperthite (c.20%)	Albite, sanidine, microperthite, orthoclase, quartz (<8%)	Quartz, oligoclase, orthoclase, perthite, sanidine and biotite (c.20%)
Lithics	Lava, tuff and rare granite	Rare	Rare	Rare
Glass / pumice	Rare	Common	Common	Rare
Fabric	Massive to crudely bedded	Non-welded to welded	Flow-banded and densely welded	Non-welded to densely welded

	Cheung Chau Suite (143 Ma)	Lion Rock Suite (141 Ma)	
		Granite Subsuite	Quartz Monzonite Subsuite
Colour	Light grey or pink	Pale pink or grey	Light pinkish white to greyish white
Rock type	Biotite monzogranite	Biotite monzogranite	Quartz monzonite
Texture	Porphyritic medium-grained	Equigranular medium-grained to fine-grained	Porphyritic medium-grained
Feldspars	Zoned oligoclase, perthitic orthoclase	Microperthite, albite, zoned oligolcase,	Orthoclase, albite
Mafic minerals	Biotite	Biotite	Hornblende, biotite
Accessory minerals	Zircon, apatite, Fe-oxide, ± titanite, ± allanite	Zircon, Fe-oxide, ± apatite, ± titanite, ± allanite	Zircon, allanite, apatite, Fe-oxide, ± titanite